PAPER

Ultrafast heating-induced magnetization switching in ferrimagnets

IOP Publishing Journal of Physics: Condensed Matter
J. Phys.: Condens. Matter **28** (2016) 476007 (10pp) doi:10.1088/0953-8984/28/47/476007

Ultrafast heating-induced magnetization switching in ferrimagnets

V N Gridnev

Ioffe Physical Technical Institute RAS, 194021 St. Petersburg, Russia

E-mail: gridnev@mail.ioffe.ru

Received 29 February 2016, revised 12 May 2016
Accepted for publication 12 May 2016
Published 26 September 2016

Abstract

We study theoretically the light-induced magnetization switching in a binary ferrimagnet of the type $A_p\,B_{1-p}$, randomly occupied by two different species of magnetic ions. The localized spins are coupled with spins of itinerant electrons via *s-d* exchange interaction. Model parameters are chosen so that to achieve similarity between magnetic characteristics of the model and those of ferrimagnetic rare-earth-transition metal GdFeCo alloys. The switching is triggered by heating of the itinerant electrons by a laser pulse. The spin dynamics is governed by the cooling of itinerant electrons, exchange scattering, induced by the *s-d* exchange interaction and spin-lattice relaxation of the itinerant spins with a characteristic time τ_s. The dynamics of the localized and itinerant spins is described by coupled rate equations. The main conclusion of this study is that the switching occurs only in a certain temperature range depending on τ_s. For long τ_s the switching occurs only below the magnetisation compensation temperature T_K. For physically reasonable values of τ_s this temperature range extends from 0 K to $T_f\,(\tau_s)$, where $T_f\,(\tau_s)$ is slightly higher than the compensation temperature T_K. With further decrease of τ_s this temperature range shifts to temperatures higher than T_K.

Keywords: all-optical, ultrafast, heating-induced, magnetization switching

(Some figures may appear in colour only in the online journal)

1. Introduction

Since the discovery of all-optical helicity dependent magnetization switching (AOS) in ferrimagnetic rare-earth-transition metal (RE-TM) amorphous GdFeCo alloy film [1, 2], this phenomenon attracts a lot of attention. However, microscopic mechanisms driving AOS are still poorly understood.

Originally [2], AOS was explained by a combined effect of femtosecond laser heating of conduction electrons to a strongly nonequilibrium state and an effective magnetic field of unknown microscopic origin, caused by a circularly polarized pump pulse. However, subsequent experiments [3, 4] showed, that AOS can be achieved without the laser-induced effective magnetic field due to the ultrafast heating alone.

Most of theoretical papers devoted to AOS use models of localized spins, coupled by exchange interactions [5–7]. These theories do not consider electron-spin coupling explicitly and thus unable to describe properly the energy and angular momentum transfer between itinerant electrons and localized spins. Though these papers demonstrate possibility of heating-induced switching in ferrimagnets, they do not give any information about microscopic mechanisms of AOS. In order to understand these mechanisms it is necessary to go beyond the framework of the approaches, which operate with macroscopic magnetizations.

In ferromagnets the magnetization dynamics is mostly determined by the temporal dynamics of the electron temperature. In ferrimagnets the dynamics is more complicated. As is pointed out in [3, 8], a distinctive features of laser-induced spin dynamics in ferrimagnets is the exchange-driven magnetization relaxation. The essence of this type of relaxation is a fast angular momentum transfer between sublattices of ferrimagnet. The exchange relaxation significantly accelerates the demagnetization of both sublattices and allows to reach a state with a small magnetization. Thus, a consistent theoretical analysis of the exchange relaxation is a key to understand AOS in ferrimagnets. A stating point of such analysis is

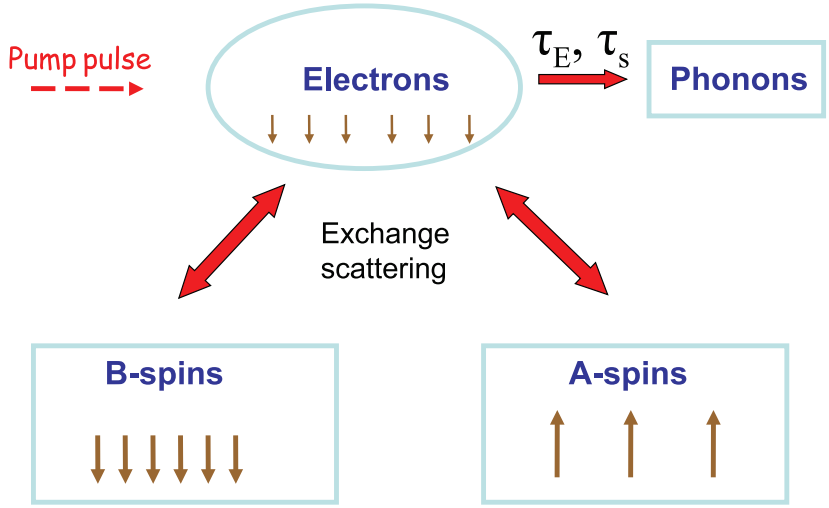

Figure 1. Different spin subsystems that participate in the energy and angular momentum exchange in the two-sublattice ferrimagnet. Photocarriers created by light transfer their energy and angular momentum to the localized spins and to the lattice. The exchange scattering channels for the energy and angular momentum transfer from the photocarriers to the localized spins system are shown by double arrows.

a choice of microscopic model accounting for a partial delocalization of electron spins.

In magnetic metals the itinerant spins are not necessarily in equilibrium with localized ones. Such a situation occurs when a magnetic metal is exposed to a femtosecond laser pulse. Since a laser pulse initially heats up itinerant electrons rather then localized spins it destroys the equilibrium between these spin subsystems. For this reason the ultrafast dynamics of both itinerant and localized spins should be considered on equal footing. Due to complexity of electronic structure of magnetic metals, the choice of an appropriate model is not straightforward.

A step forward along this line has been recently done by Baral and Schneider [9] who used a model of the ferrimagnetic RE-TM alloy, which includes two spin subsystems: localized spins antiferromagnetically coupled to an itinerant carrier system with a Stoner gap. This study shows that the exchange relaxation provides the essential contribution to AOS and the switching occurs only in ferrimagnets with a compensation point in the equilibrium magnetization.

In our study we model the RE-TM ferrimagnet by two sublattices of localized spins, interacting with itinerant electrons via the *s-d* exchange interaction, (figure 1). The essence of the *s-d* model is a sharp separation into two distinct types of electronic states: localized and delocalized (itinerant). The fundamental mechanism underlying ferromagnetic ordering in the *s-d* model is the exchange coupling between localized and delocalized spins [10–13]. This model allows to investigate processes, where an interplay between energy and spin transfer is essential. Cywiński and Sham were the first who applied the *s-d* model to the analysis of the laser-induced demagnetization in ferromagnets [14]. However, in ferromagnets the exchange scattering does not contribute significantly to the demagnetization [15], since the spin density of itinerant electrons is homogeneously distributed over unit cells (within Zener model) and significantly less than the spin density of localized spins. In ferrimagnets, the spin density of itinerant electrons, averaged over a crystal unit cell, is also small. Despite this, the itinerant spins effectively transfer the angular momentum between antiferromagnetically coupled sublattices due to an inhomogeneous distribution of itinerant spins over unit cells.

Note, that it is not obvious to consider the spins of transition-metal ions as localized. The localized vs. itinerant behaviour of transition-metal ferromagnets has been a basic problem of metallic magnetism since the 1950s. Now it is established that at zero temperature many properties of TM are explained well by the band model of 3d electrons. However, local moment models in which 3d electrons behave as the Heisenberg spins are more suited for the explanation of finite temperature equilibrium and especially nonequilibrium properties of TM. The choice of the *s-d* model allows us to study the ultrafast dynamics at finite temperatures and take into account the presence of band electrons.

In our model (figure 1) we neglect the spin-lattice relaxation of localized spins in order to show clearly a distinctive role of the spin-lattice relaxation of itinerant spins in the switching. It is known [5, 16], that the longitudinal dynamics of localized spins, which takes into account the spin-lattice relaxation, is unable to describe the switching. In contrast, in this paper we show that inclusion in the model of free electrons allows us to explain the switching of the magnetization considering only the longitudinal spin dynamics. Moreover, it turns out that the temperature dependence of the switching depends on the spin-lattice relaxation time τ_s. Note, that ignoring the spin-lattice relaxation of localized spins is not a rough approximation. Since the paper by Mitchel [17], the dominant view is that in magnetic metals the loss of energy and angular momentum from localized spins is mostly determined by the *s-d* interaction combined with the relaxation of itinerant spins to the lattice.

We will not consider the influence of the spin transport on the spin dynamics, because the relative importance of the transport depends on a sample design and laser spot size.

The paper is organized as follows. In section 2 we introduce the *s-d* model for the two-sublattice ferrimagnet and

provide equations governing the dynamics of localized and itinerant spins. In section 3 we present solutions of kinetic equations for the spin polarizations of itinerant and localized spins and demonstrate the existence of heating-induced magnetization switching. We discuss how the initial temperature and spin relaxation of carriers influence the switching process. Section 4 concludes the paper.

2. Theory

2.1. s-d model of a two-sublattice ferrimagnet

Following [14] we consider a system of localized spins embedded in a degenerate electron gas of density n_c, forming a single band with energy $E_{\mathbf{k}s}$, where $\mathbf{k}$ and s are the wave vector and spin, respectively. In equilibrium the populations of itinerant electrons for both spin directions are described by a Fermi–Dirac distribution with the temperature T and chemical potential μ.

The exchange interaction between itinerant spins $\mathbf{s}_j$ and localized spins $\mathbf{S}_i$ is given by

$$\hat{H}_{sd} = \sum_{i,j} \alpha_i \delta\left(\mathbf{r}_j - \mathbf{R}_i\right)\left(\hat{\mathbf{S}}_i \cdot \hat{\mathbf{s}}_j\right), \tag{1}$$

where $\mathbf{r}_j$ ($\mathbf{R}_i$) is the position of the carrier (localized spin) and α_i is the exchange coupling constant of the *s-d* interaction for spin $\mathbf{S}_i$. A localized spin $\mathbf{S}_i$ possesses $(2S_i + 1)$ discrete energy levels. This model is commonly referred to as *s-d* (*s-f*) model. In the following we assume that all average localized spins are parallel or antiparallel to the z axis. We will neglect orbital magnetism of the magnetic ions, i.e. we set $\langle \hat{\mathbf{L}}_i \rangle = 0$.

Experimental studies of the switching show that this is purely longitudinal process, i.e. there is no macroscopic spin procession. Hence $\langle \hat{S}_i^z \rangle \neq 0$, while $\langle \hat{S}_i^x \rangle = \langle \hat{S}_i^y \rangle = 0$. This means that the part of the *s-d* interaction containing $\hat{S}_i^z$ can be considered in the mean-field approximation, while the remaining part describes spin fluctuations. With the identity $\hat{\mathbf{S}}_i \cdot \hat{\mathbf{s}}_j = 1/2\,(\hat{S}_i^+ \hat{s}_j^- + \hat{S}_i^- \hat{s}_j^+) + \hat{S}_i^z \hat{s}_j^z$, where $\hat{S}_i^{\pm}$ and $\hat{s}_j^{\pm}$ are the localized and itinerant spin raising and lowering operators, respectively, $\hat{H}_{sd}$ can be decomposed into two parts: a dynamical part is proportional to $(\hat{S}_i^+ \hat{s}_j^- + \hat{S}_i^- \hat{s}_j^+)$, allowing for the transfer of angular momentum between the localized and itinerant spins and a static part is proportional to $\hat{S}_i^z \hat{s}_j^z$, affecting the energies of the spin systems.

Treating the diagonal part of the *s-d* interaction in a mean-field approximation, we represent $\hat{H}_{sd}$ as [14]

$$\hat{H}_{sd} = \hat{H}_{sd}^{\mathrm{mf}} + \hat{H}'_{sd}, \tag{2}$$

where

$$\hat{H}_{sd}^{\mathrm{mf}} = \sum_i \alpha_i n_c \left[\langle \hat{s}^z(\mathbf{R}_i)\rangle \hat{S}_i^z + \langle \hat{S}_i^z \rangle \hat{s}^z(\mathbf{R}_i)\right], \tag{3}$$

$$\hat{H}'_{sd} = \frac{1}{2} \sum_i \alpha_i n_c \left[\hat{S}_i^+ \hat{s}^-(\mathbf{R}_i) + \hat{S}_i^- \hat{s}^+(\mathbf{R}_i)\right], \tag{4}$$

where n_c is the density of itinerant electrons and $\hat{\mathbf{s}}(\mathbf{R}_i) = n_c^{-1} \sum_j \hat{\mathbf{s}}_j \delta\left(\mathbf{r}_j - \mathbf{R}_i\right)$ is a reduced spin density. When the itinerant spins are homogeneously distributed in space (Zener model), the average $\langle \hat{s}^z\left(\mathbf{R}_i\right)\rangle$ is exactly the average electron spin s_z along the z axis. $\hat{H}_{sd}^{\mathrm{mf}}$ is diagonal in $\hat{S}^z$ basis, while $\hat{H}'_{sd}$ is off-diagonal. The second term in the right hand side of equation (3) determines a modification of wave functions and band energies of the itinerant electrons due to magnetic ordering. As in ferromagnets [14], the quantity

$$\delta_i = n_c \alpha_i \langle \hat{s}^z\left(\mathbf{R}_i\right)\rangle, \tag{5}$$

is the energy level splitting of the localized spin at $\mathbf{R}_i$.

Below T_{C} the equilibrium values of the localized and itinerant spins obey the relation

$$s_z(R_i) = \sum_j \chi_{ij} S_j^z, \tag{6}$$

where $S_j^z \equiv \langle \hat{S}_j^z \rangle$ and $s_z(R_i) \equiv \langle \hat{s}^z(R_i)\rangle$ are the average localized spin and reduced carrier spin density at R_i, respectively, and χ_{ij} is an electron spin susceptibility. χ_{ij} can be calculated only in simplified models; RKKY model is the most known example [18]. Note, that $\chi_{ij} \propto \alpha_j$ and, hence, $\chi_{ij} \neq \chi_{ji}$ if the indices i and j refer to different magnetic sublattices, since $\alpha_j \neq \alpha_i$ in that case.

The above consideration is applicable to an arbitrary collinear magnetic structure. Now we go over to a model of two-sublattice ferrimagnet. We will study AOS in a binary ferrimagnet of the type $A_p B_{1-p}$, randomly occupied by two different species of magnetic ions with spins $S_A = 3$ and $S_B = 1$ (in units of $\hbar$), respectively.

We use here the simplest disorder model of the two-sublattice ferrimagnet, a lattice-impurity model [19, 20], and assume homogeneous distribution of average spins over cites of each magnetic sublattice, i.e. $S_{j_\nu}^z = S_\nu^z$ and $s_z\left(R_{j_\nu}\right) = s_z\left(R_\nu\right)$ for all j_ν, where $\nu = A$ or B. Then (6) can be rewritten as

$$s_z(R_\nu) = \sum_\mu S_\mu^z \sum_{j_\mu} \chi_{j_\nu j_\mu}, \tag{7}$$

where R_ν denotes an arbitrary site in the sublattice ν. It follows from this equation that the sum $\sum_{j_\mu} \chi_{j_\nu j_\mu}$ does not depend on j_ν for a given ν. Further, we assume that the distribution of A and B ions is completely uncorrelated. Then the sum over j_μ in (7) can be represented as

$$\sum_{j_\mu} \chi_{j_\nu j_\mu} = c_\mu \chi_{\nu\mu}, \tag{8}$$

where c_μ is the concentration of μ ions, $c_A = p$ and $c_B = 1 - p$. Within this simplified disorder model (6) takes the form

$$s_z\left(R_A\right) = p\chi_{AA} S_A^z + (1-p)\,\chi_{AB}\, S_B^z, \tag{9}$$

$$s_z\left(R_B\right) = p\chi_{BA} S_A^z + (1-p)\chi_{BB}\, S_B^z. \tag{10}$$

As opposed to χ_{ij}, the parameters χ_{AA}, χ_{BB}, χ_{AB}, and χ_{BA} depend on coordination numbers of the lattice sites.

It is very difficult to calculate the electron spin susceptibility χ_{ij} with sufficient accuracy for real magnetically

ordered crystals. This is even more true for the amorphous RE-TM alloys. For this reason we consider the susceptibilities χ_{AA}, χ_{BB}, χ_{AB}, and χ_{BA} as input parameters and choose their values so that to reproduce qualitatively the equilibrium magnetic characteristics of the RE-TM alloys. Therefore, we do not specify the relative arrangement of the localized spins in space. The explicit choice of physical lattice could be essential when one studies the influence of the disorder on the dynamics. For the simplest disorder model, that we use in this study, only the concentrations of TM and RE ions is essential, but not a particular choice of physical lattice. We believe that this oversimplified model of the disorder is sufficient to study microscopic mechanism of the switching. Note, however, that certain details of the switching process can be sensitive to the type of disorder (amorphization) [21].

The mean-field equations for the average localized spins S_ν^z read

$$S_\nu^z = S_\nu B_{S_\nu}\left(S_\nu \frac{\delta_\nu}{k_B T}\right), \tag{11}$$

where B_{S_ν} is the Brillouin function, T is the temperature, and $\delta_\nu = n_c \alpha_\nu s_z(\mathbf{R}_\nu)$.

The mean-field part of the exchange interaction leads to a magnetic ordering below a Curie temperature T_C. Using the standard technique we obtain from (11) the common Curie temperature for the A and B sublattices

$$T_C = Q_A\chi_{AA} + Q_B\chi_{BB} + \sqrt{(Q_A\chi_{AA} - Q_B\chi_{BB})^2 + Q_A Q_B \chi_{AB}^2}, \tag{12}$$

where $Q_\nu = \frac{1}{6} c_\nu S_\nu (S_\nu + 1) n_c \alpha_\nu$ with $c_A = p$ and $c_B = 1 - p$.

For the following discussion we introduce spin polarizations of the sublattices, $P_A = pS_A^z$, $P_B = (1-p)S_B^z$ and their sum $P = P_A + P_B$.

For numerical estimates we use the following parameter values: $\chi_{AA} = \chi_{BB} = 1, \chi_{AB} = -1, \chi_{BA} = -0.1$, $n_c = 10^{23}$ cm^{-3}, $n_c\alpha_A = 0.01$ eV and $n_c\alpha_B = 0.1$ eV. Solving equations (11) with these parameters, we find that for the concentration p in the range $0.25 < p < 0.47$ there is a compensation point T_K, i.e. a point below T_C at which the total spin polarization of localized spins P crosses zero. T_C varies from 595 K to 450 K in this concentration range. The increase of p reduces T_C, but increases T_K. Thus, the equilibrium properties of our model are qualitatively similar to those of the RE-TM ferrimagnetic alloys [19]. Note, that the functions $P_A(T)$, $P_B(T)$, $T_C(p)$, and $T_K(p)$ can be also calculated on the basis of the Heisenberg model with the Hamiltonian $\hat{H} = -\sum_{ij} J_{ij}\,\mathbf{S}_i\,\mathbf{S}_j$. Using (9) and (10) one can easily show, that within the mean-field approximation the exchange integrals between spins i and j can be expressed through the parameters of the s-d model: $z\,J_{AA} = n_c\alpha_A\chi_{AA}$, $z\,J_{BB} = n_c\alpha_B\chi_{BB}$, and $z\,J_{AB} = n_c\alpha_A\chi_{AB}$, where z is the number of nearest neighbors.

When deriving the Heisenberg Hamiltonian, electron degrees of freedom are integrated out. Typically, the spin polarization of itinerant electrons $s_z(\mathbf{r})$ is not of primary interest. The problem under study is an exception to this rule. Fortunately, the detailed knowledge of $s_z(\mathbf{r})$ is not necessary within our approach. We need only $s_z(R_A)$, $s_z(R_B)$, and $s_z = V^{-1}\int_V s_z(\mathbf{r})\,d\mathbf{r}$, the spatial average of $s_z(\mathbf{r})$. The first two quantities are given by (9) and (10), but the rigorous calculation of s_z is a complicated problem, because it requires knowledge of the wave functions and band energies of the itinerant electrons below T_C. These functions and energies are determined by the second term in (3). We define s_z from physical considerations as a linear combination of (9) and (10):

$$s_z = p\,s_z(R_A) + (1-p)s_z(R_B). \tag{13}$$

This equation gives the correct limits for Zener model of a ferromagnet ($p = 0, 1$).

Figure 2 shows the temperature dependence of the spin polarizations of localized and itinerant spins for $p = 0.35$. At this concentration $T_C = 526$ K and $T_K = 267$ K. As is seen from this figure P_A, P_B, P and $s_z(R_A), s_z(R_A), s_z$ change with temperature in a qualitatively similar manner. However, there are quantitative distinctions. While the sublattice spin polarizations P_A and P_B are quantitatively close to $s_z(R_A)$ and $s_z(R_B)$, the average spin polarizations obey the inequality $s_z \ll P$.

2.2. Kinetic equations

To describe the dynamics we extend the approach, proposed in [14] for a ferromagnetic metal, to ferrimagnets. According to this approach, the spin dynamics is governed by the exchange scattering, induced by the s-d exchange interaction, and relaxation of the itinerant spins with characteristic time τ_s (figure 1). Referring to [14] for details, we provide here only kinetic equations, governing the dynamics of interacting localized and hot itinerant spins.

After the photoexcitation the nonequilibrium electrons can be described by a Fermi–Dirac function with the electron temperature $T_e(t)$ and spin dependent chemical potentials $\mu_s(t)$:

$$f_s(E) = \frac{1}{1 + e^{(E-\mu_s)/k_B T_e}}. \tag{14}$$

The localized spins are described by populations ρ_m^ν of the Zeeman spin states, $-S_\nu \leqslant m \leqslant S_\nu$.

The populations ρ_m^ν obey the rate equations

$$\frac{d\,\rho_m^\nu}{dt} = -(w_{m-1,m}^\nu + w_{m+1,m}^\nu)\rho_m^\nu + w_{m,m+1}^\nu\rho_{m+1}^\nu + w_{m,m-1}^\nu\rho_{m-1}^\nu, \tag{15}$$

where $w_{n,m}^\nu$ is the transition rate from m to n energy level of the localized spins belonging to ν's sublattice. The average localized spins are determined by the equation $S_\nu^z = \sum_m m\rho_m^\nu$.

As is explained in the Introduction, when calculating $w_{n,m}^\nu$ we take into account only the s-d interaction. The transition rates (see appendix) are given by

$$w_{m,m\pm1}^\nu = C_\nu S_{m,m\pm1}^{\nu\mp}\frac{\beta_e(\pm\delta_\nu + \mu_s - \mu_{s'})}{1 - \exp[\beta_e(\mp\delta_\nu - \mu_s + \mu_{s'})]}, \tag{16}$$

where $S_{m,m\pm1}^{\nu\mp} = S_\nu(S_\nu+1) - m(m\pm1)$, $s = \mp\frac{1}{2}$, $s' = \pm\frac{1}{2}$, and $\beta_e = 1/k_B T_e$. The coefficients C_ν can be calculated only in simplified models [22]. For this reason we will consider C_ν

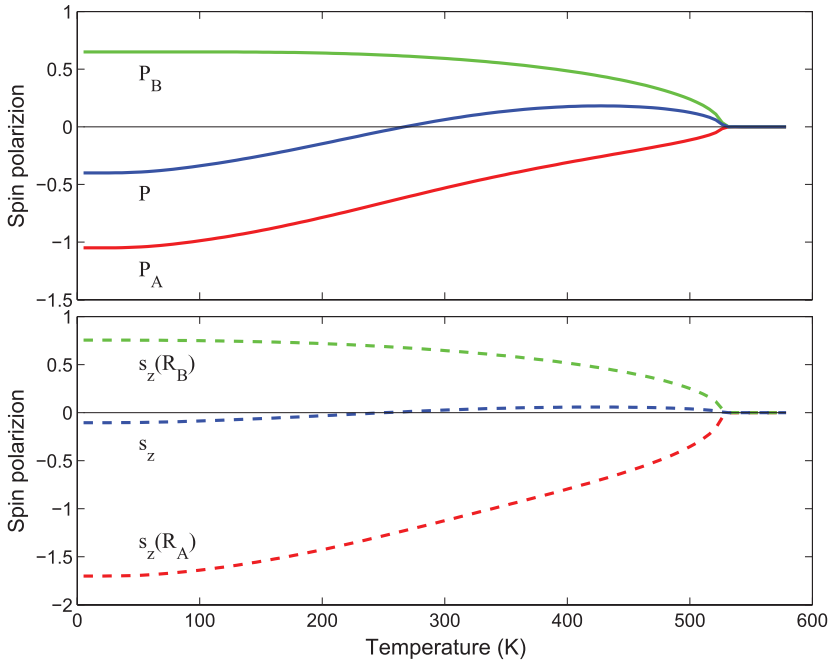

Figure 2. Calculated equilibrium spin polarization of localized (top panel) and itinerant (bottom panel) spins in A_pB_{1-p} ferrimagnetic alloy as a function of temperature for $p = 0.35$. The other parameters are provided in the main text.

as input parameters. Having in mind the RE-TM alloys, we assume that $C_B \gg C_A$.

In (16) we neglect the contributions of ion pairs describing the correlation in the relaxation between neighbouring localized spins. These terms arise in perturbational treatment of the exchange scattering because an electron wave function spreads over many magnetic ions [22, 23]. This correlation accelerates the relaxation of localized spins when the exchange interaction between them is antiferromagnetic. This effect can be neglected when the deviation of spin system from equilibrium is small [24]. In this paper we present a non-perturbative self-consistent mean-field treatment of the exchange relaxation in ferrimagnets, which is valid for the strong deviation from equilibrium. Unlike the perturbational treatment [22, 23] the energy level splitting of a localized spin (5) depends on surrounding spins. Thus, the transition rate (16) takes into account the correlation in the relaxation between neighbouring spins.

The dynamics of the average itinerant spin is determined by the exchange scattering and spin-lattice relaxation

$$\frac{\mathrm{d}s_z}{\mathrm{d}t} = -\frac{n_A}{n_c}\frac{\mathrm{d}S_A^z}{\mathrm{d}t} - \frac{n_B}{n_c}\frac{\mathrm{d}S_B^z}{\mathrm{d}t} - \frac{(s_z - s_{\mathrm{ie}}(t))}{\tau_s}, \tag{17}$$

where n_A and n_B are the concentrations of ions A and B, respectively. In the following calculations we set $n_A/n_c = p$ and $n_B/n_c = 1 - p$. The first two terms on the right-hand side describe the exchange scattering. The form of this terms clearly reflects the conservation of the total spin of the system in the process of exchange scattering. The third term describes the spin-lattice relaxation of the average electron spin with a relaxation time τ_s. Here $s_{\mathrm{ie}}(t)$ is an instantaneous equilibrium value of the average electron spin s_z, determined by the electron temperature T_e and by the condition $\mu_\uparrow = \mu_\downarrow$. We define s_{ie} similar to (13):

$$s_{\mathrm{ie}}(t) = p\, s_z(R_A, t) + (1 - p)s_z(R_B, t), \tag{18}$$

where $s_z\,(R_A)$ and $s_z\,(R_B)$ are given by (9) and (10) with time-dependent S_A^z and S_B^z. An important role of equation (18) is that it makes the rate equations (15) and (15) coupled.

We stress again, that the spin relaxation time τ_s in (15) does not include contribution from the exchange-scattering processes, because the first two terms on the right-hand side in (15) already take into account these processes. It seems reasonable to suppose that τ_s is in the range from 10 fs to 1 ps.

More strong coupling between the dynamics of the itinerant and localized spins arises due to a dependence of the spin splitting of the carriers' chemical potential $\Delta\mu = \mu_\uparrow - \mu_\downarrow$ on $S_A^z\,(t)$, $S_B^z\,(t)$, and $s_z(t)$. Using the definition

$$n_s = \int f_s(E) D_s(E)\,\mathrm{d}E, \tag{19}$$

and taking into account that $s_z = \frac{1}{2}(n_\uparrow - n_\downarrow)$ and $n_c = (n_\uparrow + n_\downarrow)$ one can easily obtain

$$\mu_\uparrow - \mu_\downarrow = n_c(s_z - s_{\mathrm{ie}})\frac{D_\uparrow\,(E_\mathrm{F}) + D_\downarrow\,(E_\mathrm{F})}{D_\uparrow\,(E_\mathrm{F})\,D_\downarrow\,(E_\mathrm{F})}. \tag{20}$$

Here $D_s(E_\mathrm{F})$ is the spin-resolved density of states at the Fermi level.

To make equations (15) and (15) closed one should supplement it with an equation for the electron temperature $T_\mathrm{e}(t)$. We model the time dependence of T_e by an equation

$$T_\mathrm{e} = T + \Delta T_\mathrm{e}\,(1 - \mathrm{e}^{-t/\tau_0})\mathrm{e}^{-t/\tau_\mathrm{E}}, \tag{21}$$

where ΔT_e is the sharp increase of the electron temperature, τ_0 is the risetime of the electron temperature to its maximum value and τ_E is the energy relaxation time of the itinerant electrons.

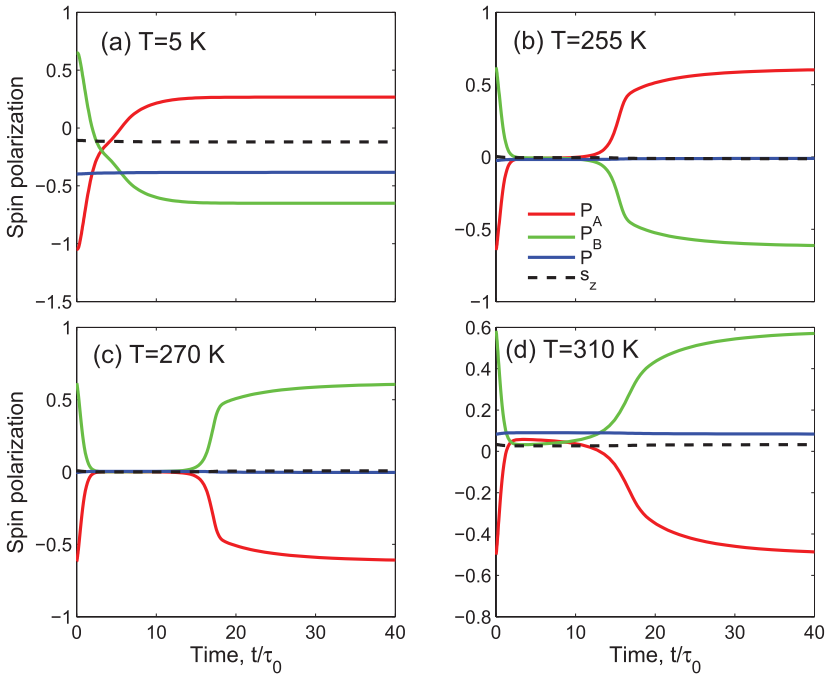

Figure 3. Computed dynamics of localized and itinerant spins in $A_{35}B_{65}$ without the spin-lattice relaxation ($\tau_s = \infty$) for different initial temperatures below ((a), (b)) and above ((c), (d)) compensation temperature $T_K \approx 267$ K. The peak electron temperature $T_{max} = 1.5\ T_C$.

Since the equilibration time of itinerant electrons is rather short (∼10 fs), the risetime τ_0 is close to the pulse duration time (∼ 100 fs). The energy relaxation time τ_E is of the order of several picoseconds, i.e. $\tau_0/\tau_E \ll 1$. It can be easily shown from (21) that the maximum electron temperature $T_{max} \approx T + \Delta T_e$.

In metals, the rise in lattice temperature due to heat transfer from the carriers is small (for $T_{max} \sim 1000$ K), and can be neglected. For this reason we assume that $T_e(t)$ approaches the initial temperature T on the time scale $\sim \tau_E$.

Thus, the nonequilibrium state is characterized by the average localized and itinerant spins, $S_\nu^z(t)$, $s_z(t)$, and the electron temperature $T_e(t)$. Equation (20) defines the spin splitting of the chemical potential $\mu_\uparrow - \mu_\downarrow$ as a function of the average spins.

3. Results

Numerical solution of the nonlinear equations (15) and (15) shows that the time dependence of S_ν^z and s_z is determined by a complicated interplay of the parameters entering these equations. For this reason, here, we focus only on the most important features of the dynamics and consider the time dependence of the sublattice spin polarizations on the initial temperature and spin relaxation time of itinerant electrons. The exchange scattering rates and electron temperature are given by (16) and (21), respectively, where we set $C_A = \tau_0^{-1}$, $C_B = 10\tau_0^{-1}$, and $\tau_E = 10\tau_0$.

3.1. No spin relaxation

As a stating point it is instructive to consider the dynamics in a nonphysical situation when the spin-lattice relaxation of the itinerant electrons is absent, i.e. $\tau_s = \infty$. In this case the total angular momentum of the localized and itinerant spins $P_A + P_B + s_z$ is conserved. Figure 3 shows the dependence of the spin polarizations on the reduced time, t/τ_0, for different temperatures. One can see a qualitative difference between temporal behavior of P_ν below and above the compensation temperature T_K (≈267 K). Below T_K (figures 3(a) and (b)) both P_A and P_B change their signs with time and approach to quasi-equilibrium values. In this process $P_A + P_B \approx$ const., since $s_z \ll P_A + P_B$. Such process is not the switching in the strict sense. We will call it as incomplete switching. Above T_K temporal behavior of P_ν is qualitatively different: after a strong reduction, P_ν return to the initial values (figures 3(c) and (d)). Thus, one can see that the exchange scattering alone, without the spin-lattice relaxation, is more effective in the angular momentum transfer between the sublattices below T_K.

To understand the reason for the asymmetry in the temporal behavior of P_ν relative to the compensation point, we note that the spin splitting of B spins (TM) significantly exceeds that of A spins (RE), i.e. $|\delta_B| \gg |\delta_A|$. As a consequence, due to energy and angular momentum conservation the exchange scattering is more effective when $|P_B| < |P_A|$, that is, below T_K.

Thus, the conservation of energy and angular momentum in the absence of the spin relaxation prevents the switching. To overcome the limitations imposed on the dynamics by the conservation laws, the spin-lattice relaxation of the itinerant electrons must be turned on.

3.2. Slow spin relaxation

Based on the above consideration we expect that when the spin relaxation rate increases the switching appears first below T_K. Numerical calculations with relatively slow spin relaxation,

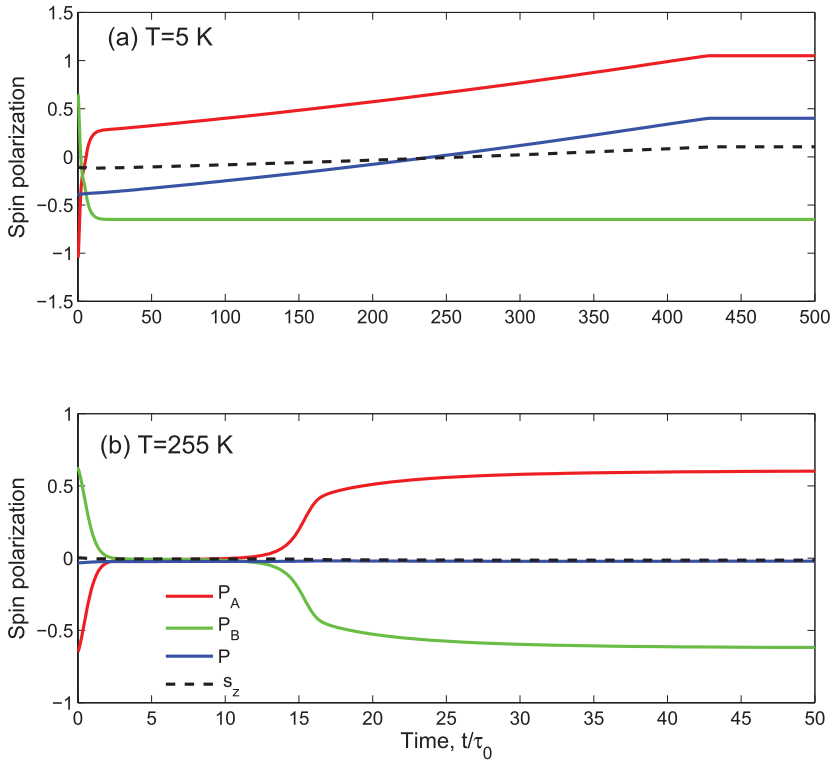

Figure 4. Ultrafast switching of the spin polarizations P_A, P_B, P and s_z for initial temperatures below the compensation temperature, with the electron-spin relaxation time $\tau_s = \tau_0$. The parameters p, $T_{\max}$ and T_K are the same as in figure 3.

$\tau_s = \tau_0$, confirm this assumption, see figure 4. Above T_K the switching is still absent (not shown). Comparison of figures 3(a) and 4(a) allows us to understand better the role of the exchange scattering and spin relaxation in the switching. Immediately after the photo-excitation the exchange scattering causes the relatively fast angular momentum transfer between the sublattices until the complete switching of B sublattice. This asymmetry in behaviour of A and B sublattices is due to the inequality $|P_B| < |P_A|$ at low temperatures. As is seen from figures 3(a) and 4(a), duration of this stage ($\sim 10\tau_0$) is the same both without and with the spin relaxation. Without the spin relaxation the first stage is also a final stage because the sublattice spin polarizations remain unchanged over time (figure 3(a)). If the relaxation of itinerant spins occurs, the A sublattice continues the switching until it switches completely on a longer time scale $\simeq 430\tau_0$ (figure 4(a), red line). Thus, at slow spin relaxation and low temperatures the complete reversal of A and B sublattices occurs on distinctly different timescales. When the initial temperature approaches the compensation point, P_B approaches P_A and the switching times of both sublattices become comparable.

Without the spin relaxation the net spin polarization $P_A + P_B$ is conserved (figure 3) and the switching, i.e. the process $(P_A + P_B) \to -(P_A + P_B)$, is impossible. However, near the magnetic compensation point $(P_A + P_B) \approx 0$ the processes $P_A \to \approx -P_A$ and $P_B \to \approx -P_B$ (figure 3(b)) is almost indistinguishable from the true switching $P_A \to -P_A$ and $P_B \to -P_B$ (figure 4(b)). For this reason the figures 3(b) and 4(b) show similar behavior.

3.3. Fast spin relaxation

Decrease of τ_s changes the temperature and time dependencies of the switching. Figure 5 shows the calculated dynamics with $\tau_s = 10^{-2}\tau_0$. Now the switching appears above T_K (figure 5(c)) and exists up to a temperature T_f, $T_K < T_f < T_C$; T_f depends on parameters of the model. Varying these parameters we were unable to get $T_f > 340$ K (for $\tau_s = 10^{-2}\tau_0$). Above T_f the switching disappears (figure 5(d)). In contrast to the slow spin relaxation (see section (3.2)), the temporal behaviours of the switching below and above T_K do not differ qualitatively.

With further decrease of τ_s the switching occurs only at temperatures above T_K. Figure 6 shows the dynamics at different temperatures with $\tau_s = 10^{-3}\tau_0$. As is seen from this figure the switching disappears bellow T_K, but arises above T_K and occurs up to the critical temperature T_C. The temperature dependence of the switching at $T > T_K$ is non-monotonous: at $T = 310$ K and 500 K the magnetization switches, but at $T = 400$ K it recovers. Currently, we have no convincing explanation of such non-monotonous temperature behavior of the switching. As is seen from (16), the transition rates $w^{\nu}_{m,m\pm1}$ are determined by coupled nonlinear dynamics of the three spin subsystems. This complicates the interpretation of all features of the dynamics in simple physical terms. Note, that the spin relaxation time $\tau_s = 10^{-3}\tau_0 \approx 0.1$ fs too small for real materials and, probably, the behavior, shown in figure 6 can not be observed in real experiments.

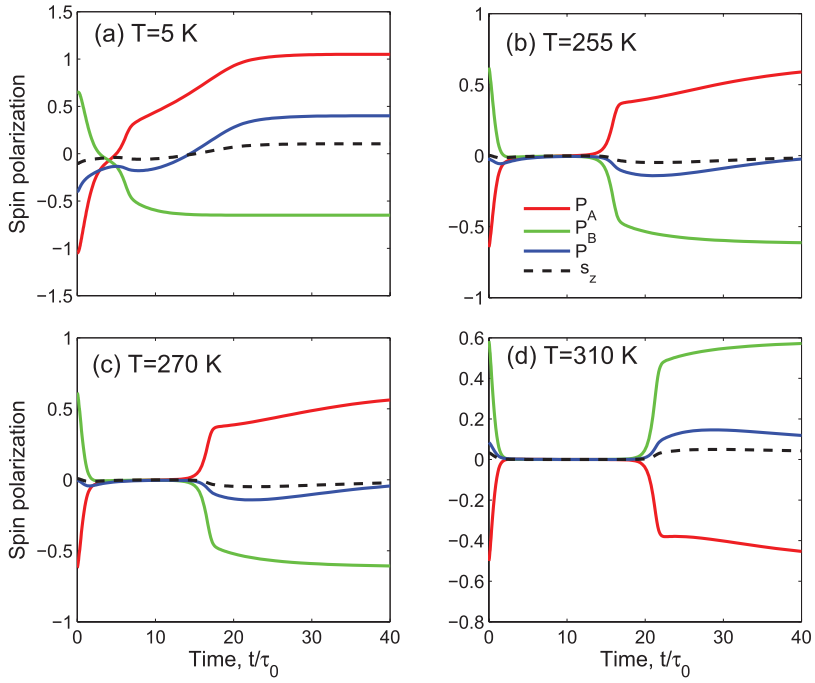

Figure 5. Ultrafast switching ((a)–(c)) and demagnetization (d) for various initial temperatures, with the electron-spin relaxation time $\tau_s = 10^{-2}\tau_0$. The parameters p, $T_{\max}$ and T_K are the same as in figure 3.

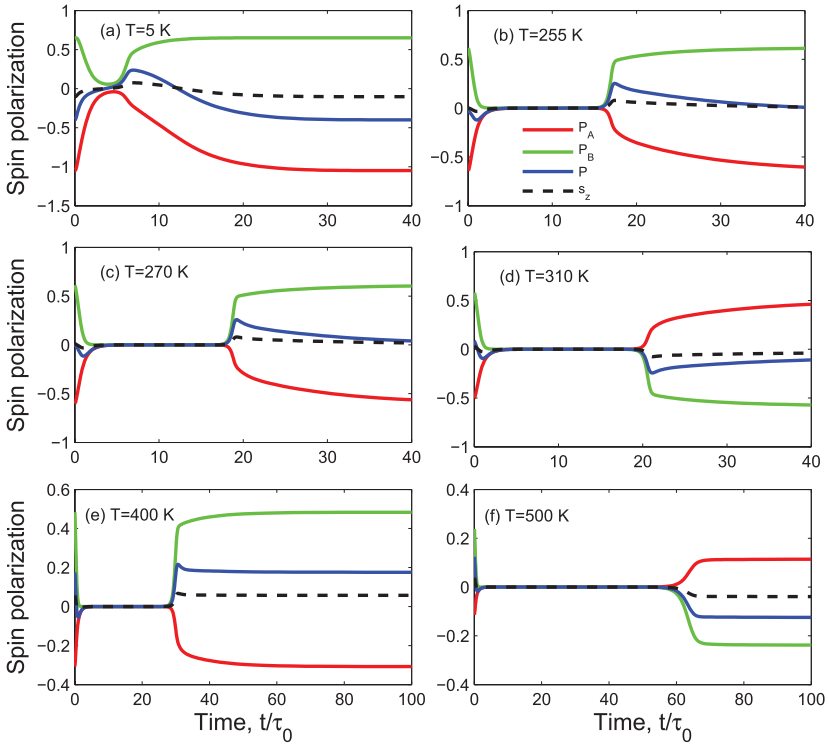

Figure 6. Ultrafast switching (d), (f) and demagnetization (a), (b), (c), (e) for various initial temperatures, with the electron-spin relaxation time $\tau_s = 10^{-3}\tau_0$. The parameters p, $T_{\max}$ and T_K are the same as in figure 3.

4. Discussion and conclusions

We have presented a theoretical study of the heating-induced all-optical magnetization switching in the two-sublattice ferrimagnet. More specifically, our purpose was to go beyond the framework of models based on localized spins in order to investigate the angular momentum transfer between the sublattices more thoroughly. To this end we choose the model, which comprises three spin species: two sublattices of localized spins, interacting with itinerant spins via the *s-d* exchange interaction. The spin dynamics is governed by two different processes: spin transfer between the localized and

itinerant spins due to the *s-d* exchange interaction and spin-lattice relaxation of itinerant spins.

Our model does not take into account many features of real RE-TM ferrimagnets. Among them we notice only those, which, in principle, can be accounted for within the *s-d* model.

We do not study the influence of type of disorder and amorphization on the switching. Disorder always prevents the emergence of collective phenomena. Since magnetism and the magnetization switching are collective phenomena, one can expect that disorder is not favorable for the switching. This seems to be true for our model in which transfers components of the sublattice magnetizations are not operative. For this reason, in this manuscript we focus on the microscopic mechanism of the switching and choose the simplest model of disorder. However, if the transfers components of the sublattice magnetizations play an essential role in the switching mechanism [5], the chemical inhomogeneity of the amorphous RE-TM ferrimagnets can be crucial for the switching.

We do not take into account a magnetocrystalline anisotropy although the real GdFeCo films have the perpendicular magnetic anisotropy. The anisotropy affects the energy levels of localized spins and thus affects the dynamics. However, the anisotropy is not responsible for the collective phenomena such as angular momentum transfer between the RE and TM sublattices. Therefore, the anisotropy is not crucial for the switching. In case of strong anisotropy its effect can be reduced by increasing the pump pulse energy (similarly to heat-assisted magnetic recording).

Finally, we note that our model ignores an orbital contribution to magnetism. There is no simple generalization of the *s-d* model to magnetic materials, containing RE and/or TM ions with non-zero orbital angular momentum [13]. This creates an additional difficulty in the interpretation of the experiments with TbCo ferrimagnetic alloys.

Despite these simplifications, we were able to choose parameters of the model so that its main equilibrium magnetic characteristics were similar to those of the RE-TM ferrimagnetic alloys. We calculated these characteristics using the *s-d* model but the same results can be obtained from the Heisenberg model. When considering equilibrium sublattice magnetizations, the *s-d* model is equivalent to the Heisenberg model. In nonequilibrium the both models become nonequivalent, since nonequilibrium itinerant spins can not be integrated out and, hence, the Hamiltonian of the *s-d* exchange interaction can not be reduced to the Heisenberg Hamiltonian. Recall that Landau–Lifshitz–Bloch equation relying on the Heisenberg Hamiltonian unable to describe the switching without spin precession [5].

The evolution of the spin subsystems after the rapid heating of itinerant electrons is described by the system of coupled rate equations. The probabilities of transitions between spin sublevels of the localized spins, $w^{\mathrm{RE}}_{n,m}$ and $w^{\mathrm{TM}}_{n,m}$, depend on the nonequilibrium spin polarizations of all three spin subsystems. This leads to the strong nonlinear coupling between them. We were able to calculate $w^{\nu}_{n,m}$ with accuracy up to numerical constants, which we consider as input parameters. Since 3 *d* electrons interact with itinerant spins more strongly than 4 *f* ones, we choose these constants so that $w^{\mathrm{RE}}_{n,m}/w^{\mathrm{TM}}_{n,m} \sim 0.1$.

Depending on parameters of the model the rate equations describe both the demagnetization and switching. As regards to the demagnetization, our rate equations and Landau–Lifshitz–Bloch equation predict qualitatively similar temporal behavior of the sublattice magnetizations. As is seen from figures 3–5, at low temperatures the *B* sublattice relaxes faster than the *A* sublattice. When the temperature increases and reaches the compensation temperature, the both relaxation rates become comparable. Similar result was obtained in [25] for the localized spin model.

Our calculations show that the dynamics of the switching strongly depends on the spin-lattice relaxation time τ_s. The switching occurs only in a certain temperature range depending on τ_s. For long τ_s the switching occurs only below the magnetisation compensation temperature T_{K}. For physically reasonable values of $\tau_s \sim (1 \div 100)$ fs this temperature range extends from 0 K to $T_f(\tau_s)$, where $T_f(\tau_s)$ is slightly higher than the compensation temperature T_{K}. With further decrease of τ_s to very small (and unphysical) values this temperature range shifts to temperatures higher than T_{K}.

Nonequilibrium itinerant spins play a key role in our theory. The spin polarization of the itinerant electrons acts on the sublattice magnetizations as an effective magnetic field. In certain parameter region this field switches partially demagnetized sublattices. We stress again that the effective magnetic field is determined by the collective dynamics of all three spin subsystems.

The switching is more efficient when the initial temperature is below T_{K}. When the initial temperature increases and goes over the compensation point T_{K} the switching gradually disappears. This conclusion qualitatively agrees with the experiments [26, 27].

Recently we became aware, that similar model of AOS was developed in [28]. The authors of that paper consider the problem of the angular momentum transfer between two nonequivalent magnetic sublattices in a ferrimagnetic metal, triggered by femtosecond laser heating of itinerant electrons. They came to the conclusion that AOS is supported by the exchange coupling of the localized spin subsystems to the electrons. However, the temperature dependence of AOS and the role of the magnetic compensation point were not addressed. Besides, there is a number of differences in mathematical details of their and our models.

Acknowledgments

This work was supported by the Russian Foundation for Basic Research (Projects 13-02-00754, 15-02-09052 and 16-02-00377), the Ministry of Education and Science of the Russian Federation (Project 14.613.21.0048)

Appendix. Exchange scattering rate

The transition rate $w^{\nu}_{n,m}$ from *m* to *n* energy level of the localized spin induced by *s-d* interaction with the carriers is given by [22]

$$w^{\nu}_{n,m} = \sum_{\mathbf{k}s,\mathbf{k}'s'} w^{\nu}_{n\mathbf{k}'s',m\mathbf{k}s} f(\mathbf{k},s)[1-f(\mathbf{k}',s')], \tag{A.1}$$

where

$$w^{\nu}_{n\mathbf{k}'s',m\mathbf{k}s} = \frac{2\pi}{\hbar}|\langle n\mathbf{k}'s'|\hat{H}^{\nu}_{sd}|m\mathbf{k}s\rangle|^2 \times \delta(E^{\nu}_m + E_{\mathbf{k}s} - E^{\nu}_n - E_{\mathbf{k}'s'}) \tag{A.2}$$

with $\hat{H}^{\nu}_{sd} = \sum_j \alpha_\nu \delta(\mathbf{r}_j - \mathbf{R}_\nu)(\hat{\mathbf{S}}_\nu \cdot \hat{\mathbf{s}}_j)$. The wave function of the localized spin $\mathbf{S}_\nu$ and an electron is

$$|m\mathbf{k}s\rangle = |m\rangle|s\rangle u_{s\mathbf{k}}(\mathbf{r})e^{i\mathbf{k}\cdot\mathbf{r}}. \tag{A.3}$$

These wave functions and corresponding energies $E^{\nu}_m + E_{\mathbf{k}s}$, $-S_\nu < m < S_\nu$, should be calculated taking into account the mean-field part of the exchange interaction. For this reason E^{ν}_m and $E_{\mathbf{k}s}$ depend on time. Since $\hat{H}^{\mathrm{mf}}_{sd}$ commutes with $\hat{s}^z$, it is allowed to choose the electron wave function as a product of a spin function $|\pm\frac{1}{2}\rangle$ and a Bloch function. Note that in a ferrimagnet the Bloch amplitude $u_{s\mathbf{k}}$ depends on the electron spin state s, since the spatial electron spin distribution essentially depends on s.

Substituting (A.2) into (A.1) and replacing $\sum_{\mathbf{k}s}$ by $\sum_s \int D_s(E)\,\mathrm{d}E$ we obtain

$$\begin{aligned} w^{\nu}_{n,m} &= \frac{\alpha^2_\nu}{4}\frac{2\pi}{\hbar} S^{\nu\mp}_{n,m} \int f_s(E)[1-f_{s'}(E')] \\ &\quad \times |\langle \mathbf{k}'s'|\hat{s}^{\pm}|\mathbf{k}s\rangle|^2 D_s(E) D_{s'}(E') \\ &\quad \times \delta(E^{\nu}_m + E - E^{\nu}_n - E')\mathrm{d}E\,\mathrm{d}E' \\ &= \frac{\alpha^2_\nu}{4}\frac{2\pi}{\hbar} S^{\nu\mp}_{n,m} \langle |u_{\mathbf{k}}(\mathbf{R}_\nu)|^2\rangle^2_{E_\mathrm{F}} \int [1-f_{s'}(E\pm\delta_\nu)] \\ &\quad \times f_s(E) D_s(E) D_{s'}(E\pm\delta_\nu)\mathrm{d}E, \end{aligned} \tag{A.4}$$

where $S^{\nu\mp}_{m,m\pm1} = S_\nu(S_\nu - 1) - m(m\pm1)$, $m = n \pm 1$, $s = \mp\frac{1}{2}$, $s' = \pm\frac{1}{2}$, and $\langle |u_{\mathbf{k}}(\mathbf{R}_\nu)|^2\rangle_{E_\mathrm{F}}$ is the average of $|u_{\mathbf{k}}(\mathbf{R}_\nu)|^2$ over the Fermi surface.

Using the explicit forms of occupation functions, (14), we obtain from (A.4)

$$w^{\nu}_{m,m\pm1} = C_\nu S^{\mp}_{m,m\pm1} \frac{\beta_e(\pm\delta_\nu + \mu_s - \mu_{s'})}{1 - \exp[\beta_e(\mp\delta_\nu - \mu_s + \mu_{s'})]}, \tag{A.5}$$

where

$$C_\nu = \frac{\alpha^2_\nu}{4}\frac{2\pi}{\hbar}\langle |u_{\mathbf{k}}(\mathbf{R}_\nu)|^2\rangle^2_{E_\mathrm{F}} D_s(E_\mathrm{F}) D_{s'}(E_\mathrm{F}\pm\delta_\nu). \tag{A.6}$$

When deriving (A.5) we have assumed that $D_s(E)$ and $D_{s'}(E)$ are slowly varying functions near the Fermi surface.

References

[1] Stanciu C D, Hansteen F, Kimel A V, Kirilyuk A, Tsukamoto A, Itoh A and Rasing T 2007 *Phys. Rev. Lett.* **99** 047601
[2] Vahaplar K, Kalashnikova A M, Kimel A V, Hinzke D, Nowak U, Chantrell R, Tsukamoto A, Itoh A, Kirilyuk A and Rasing T 2009 *Phys. Rev. Lett.* **103** 117201
[3] Ostler T A *et al* 2012 *Nat. Commun.* **3** 666
[4] Khorsand A R, Savoini M, Kirilyuk A, Kimel A V, Tsukamoto A, Itoh A and Rasing T 2012 *Phys. Rev. Lett.* **108** 127205
[5] Atxitia U, Ostler T, Barker J, Evans R F L, Chantrell R W and Chubykalo-Fesenko O 2013 *Phys. Rev.* B **87** 224417
[6] Schellekens A J and Koopmans B 2013 *Phys. Rev.* B **87** 020407
[7] Wienholdt S, Hinzke D, Carva K, Oppeneer P M and Nowak U 2013 *Phys. Rev.* B **88** 020406
[8] Mentink J H, Hellsvik J, Afanasiev D V, Ivanov B A, Kirilyuk A, Kimel A V, Eriksson O, Katsnelson M I and Rasing T 2012 *Phys. Rev. Lett.* **108** 057202
[9] Baral A and Schneider H C 2015 *Phys. Rev.* B **91** 100402
[10] Zener C 1951 *Phys. Rev.* **81** 440
[11] Kasuya T 1956 *Prog. Theor. Phys.* **16** 45
[12] Yosida K 1957 *Phys. Rev.* **106** 893
[13] Vonsovskii S V 1974 *Magnetism* (New York: Wiley)
[14] Cywiński L and Sham L J 2007 *Phys. Rev.* B **76** 045205
[15] Gridnev V N 2013 *Phys. Rev.* B **88** 014405
[16] Suarez O J, Nieves P, Laroze D, Altbir D and Chubykalo-Fesenko O 2015 *Phys. Rev.* B **92** 144425
[17] Mitchell A H 1957 *Phys. Rev.* **105** 1439
[18] Kittel C 1987 *Quantum Theory of Solids* 2nd edn (New York: Wiley)
[19] Ostler T A *et al* 2011 *Phys. Rev.* B **84** 024407
[20] Hinzke D, Atxitia U, Carva K, Nieves P, Chubykalo-Fesenko O, Oppeneer P M and Nowak U 2015 *Phys. Rev.* B **92** 054412
[21] Chimata R *et al* 2015 *Phys. Rev.* B **92** 094411
[22] Slichter C P 1996 *Principles of Magnetic Resonance* (Berlin: Springer)
[23] Hebel L C and Slichter C P 1959 *Phys. Rev.* **113** 1504
[24] Rikitake Y and Imamura H 2005 *Phys. Rev.* B **72** 033308
[25] Atxitia U, Barker J, Chantrell R W and Chubykalo-Fesenko O 2014 *Phys. Rev.* B **89** 224421
[26] Medapalli R, Razdolski I, Savoini M, Khorsand A R, Kalashnikova A, Tsukamoto A, Itoh A, Kirilyuk A, Kimel A and Rasing T 2013 *Eur. Phys. J.* B **86** 183
[27] Vahaplar K *et al* 2012 *Phys. Rev.* B **85** 104402
[28] Kalashnikova A M and Kozub V I 2016 *Phys. Rev.* B **93** 054424